

Strength Design on Permanent Magnet Rotor in High Speed Motor Using Finite Element Method

Zhang Tao*, Ye Xiaoting, Zhang Huiping, Jia Hongyun

Faculty of Electronic and Electrical Engineering, Huaiyin Institution of Technology,

No.1 East Mei Cheng Road, tel: (+086)0517-833599052

*Corresponding author, e-mail: zhangtaohyt@126.com

Abstract

The permanent magnets can be damaged for the tremendous centrifugal stress when the permanent magnet rotor rotates in high-speed. In this paper, the mechanical strength of high-speed permanent magnet rotor was researched. Stability operation mechanical conditions of the surface-mounted permanent magnet rotor were analyzed. The mathematical model between the shrink range of bandage and the maximum operating speed were concluded. The strengths of two kinds of surface-mounted permanent magnet rotors were calculated and compared using contact finite element method. For buried type permanent magnet rotor, the equivalent ring method was put forward to calculate its stress limit. The mathematical relationships between the maximum velocity and iron bridge thickness have been deduced. Using finite element method, the stress distributions was analyzed. The research results have shown that the high speed permanent magnet rotors designed according to the method proposed here had the adequate mechanical strength.

Keywords: high speed motor, permanent magnet rotor, mechanical strength, stress, finite element analysis

Copyright © 2014 Institute of Advanced Engineering and Science. All rights reserved.

1. Introduction

With the rapid development of science, technology and productivity, high-precision tools, such as precise numerically-controlled machine tools, turbo molecular pumps, small generators and high-speed flywheel energy storage devices, are widely applied in engineering, which gives urge requirement of high-speed and super-speed motors [1, 4]. The high-speed motor has some remarkable advantages, such as: (1) It possesses smaller volume, less raw material, higher power density, and higher efficiency; (2) It can drive the load directly without the transmission mechanism, which means less transmission and noise; (3) The rotor of high-speed motor has less rotational inertia and thus has higher-speed dynamic response. For its promising application in special electrical transmission and high-speed direct-drive fields, the high-speed motor has becoming the international research topic in the electrical engineering fields [5, 6].

The AC motor with squirrel cage rotor, switched reluctance machines and permanent magnet synchronous motor are all qualified for high speed operation [7, 8]. But the permanent magnet synchronous motors are becoming more and more favored for the non-electric excitation, rotor losses are very small, leading to minor thermal rotor expansion and to an increased efficiency. However, high speed direct-drives system requires special rotor designs, especially with respect to mechanical strength issues, to be able to withstand high mechanical stress. But according to the current literature, the mechanical strength design of permanent magnet rotor has not been reported.

In this paper, stability operation mechanical conditions of the surface-mounted permanent magnet rotor are analyzed. The mathematical model between the shrink range of bandage and the maximum operating speed are concluded. The strengths of two kinds of surface-mounted permanent magnet rotors are calculated and compared using contact finite element method. For buried type permanent magnet rotor, the equivalent ring method is put forward to calculate its stress limit. The mathematical relationships between the maximum velocity and iron bridge thickness are deduced. Using finite element method, the stress distributions is analyzed. The research results have shown that the high speed permanent magnet rotors designed according to the method proposed here have the adequate mechanical strength.

2. Stability Operation Mechanical Condition

Figure 1 shows an axial cross section of a permanent magnet rotor 1 with permanent magnets glued onto the rotor surface and fixed by a carbon- or glass-fiber bandage. To achieve a defined prestress and a contact force, bandages are designed as prefabricated sleeves made from either glass or carbon-fiber. When the a circumferential speed is above 150m/s, the strength of glass-fiber bandages is not sufficient anymore to safely fix the magnets to the rotor surface. And thus, the carbon-fiber technology with maximum permissible tension of $\sigma_{t,max}=1100\text{N/mm}^2$ is a high-quality alternative. The parameters are shown in Table 1.

Table 1. Comparison of Material Properties

Material	$E_{11}(\text{Gpa})$	$E_{12}(\text{Gpa})$	Poisson's ratio	Desity(kg/m^3)	$\Sigma t(\text{Mpa})$
G-fiber	73	73	0.22	2500	860
C-fiber	135	8.8	0.199	1800	1100
Iron	211	211	0.27	7650	450

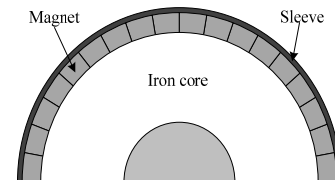


Figure 1. Structure of Permanent Magnet Rotor 1

With respect to the rotor outer diameter R_a , the sleeve has a small undersize ΔD . The assembly of the rotor is done by either axial pressing or cold shrinking of the sleeve onto the rotor. The contact force due to the glue is neglected. And thus the mechanical stress of the bandage is mainly in the form of tangential tensile stress σ_t . The bandage has to withstand centrifugal forces at 120% rated speed and must provide a positive residual contact pressure $p_{N,max}$ between the magnets and the rotor iron. It must be assured that the maximum permissible tangential stress $\sigma_{N,max}$ inside the bandage is not exceeded. These two fundamental conditions for the mechanical stability of a high-speed permanent-magnet rotor at the maximum speed are described as following.

$$\begin{cases} p_{N,max} = p_{pre} + p_{tem} - p_{\omega} > 0 \\ \sigma_{N,max} = \sigma_{pre} + \sigma_{tem} + \sigma_{\omega} < \sigma_t \end{cases} \quad (1)$$

Using Young's modulus E , the sleeve undersize ΔD , the prestress σ_{pre} and the contact pressure p_{pre} due to shrinking or pressing of the sleeve onto the rotor is given by (2).

$$\begin{cases} \sigma_{pre} = \frac{\Delta D}{R_a} E \\ p_{pre}(r) = \sigma_{pre} \left[\frac{r_i^2}{r_o^2 - r_i^2} \left(1 + \frac{r_o^2}{r^2} \right) \right]^{-1} \end{cases} \quad (2)$$

Where, r_i and r_o are the inner and outer bandage radii, respectively.

The bandage always is considered as the thin shell. The Equation (2) can be expressed by:

$$\begin{cases} \sigma_{pre} = \frac{\Delta D}{R_a} E \\ p_{pre}(r) = \sigma_{pre} \frac{h_b}{r_b} \end{cases} \quad (3)$$

Where, h_b and r_b represent height and average radius of the bandage.

The thermal expansion of bandage can be neglected. Expansion of metal rotor parts such as rotor iron and magnets will put a big strain on the bandage. The thermal expansion of magnet and iron Δd is described as following.

$$\Delta d = \alpha \Delta T R_a \tag{4}$$

The stress σ_{tem} and force p_{tem} caused by thermal expansion are expressed by (5).

$$\begin{cases} \sigma_{\text{tem}} = \frac{\Delta d}{R_a} E \\ p_{\text{tem}}(r) = \sigma_{\text{tem}} \frac{h_b}{r_b} \end{cases} \tag{5}$$

Additional tangential stress due to rotation of the bandage with mass density ρ_b at the maximum speed ω_{max} and the additional centrifugal forces on magnets and bandage each reduce the total contact pressure between rotor and magnets are given by Equation (6).

$$\begin{cases} \sigma_{\omega}(r) = 0.4125 \rho_b \omega_{\text{max}}^2 (0.424 r^2 + 2 r_o^2) \\ p_{\omega} = r_b \rho_b \omega_{\text{max}}^2 h_b \end{cases} \tag{6}$$

If the bandage is considered as the thin shell, the tangential stress depends on the radius. The Equation (6) can be described as (7).

$$\begin{cases} \sigma_{\omega}(r) = \rho_b \omega_{\text{max}}^2 r^2 \\ p_{\omega} = r_b \rho_b \omega_{\text{max}}^2 h_b \end{cases} \tag{7}$$

Then, we can conclude the stability operation mechanical conditions of permanent magnet rotor in high speed motor as following.

$$\begin{cases} \frac{\Delta D}{R_a} E + \frac{\alpha \Delta T R_a}{R_a} E + \rho_b \omega_{\text{max}}^2 r^2 < \sigma_t \\ \left(\frac{\Delta D}{R_a} + \frac{\alpha \Delta T R_a}{R_a} \right) E \left[\frac{r_i^2}{r_o^2 - r_i^2} \left(1 + \frac{r_o^2}{r^2} \right) \right]^{-1} - r_b \rho_b \omega_{\text{max}}^2 h_b > 0 \end{cases} \tag{8}$$

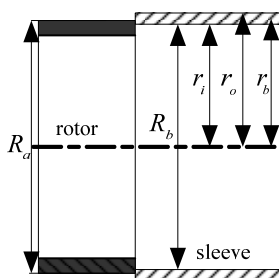


Figure 2. Parameter of Permanent Magnet Rotor

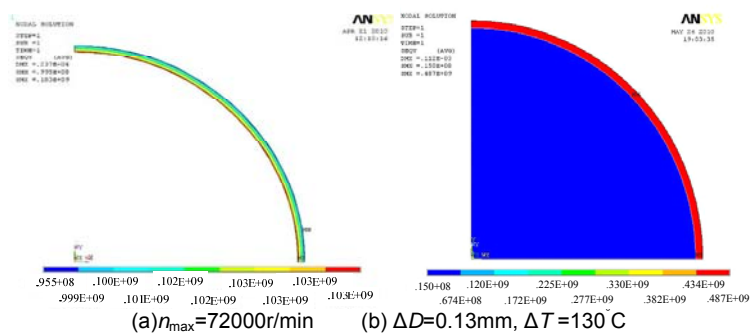


Figure 3. Stress Distribution

3. Strength Analysis of Surface Mounted Rotor

The surface-mounted permanent magnet rotor structure 1 is shown in Figure 1. The maximum speed $n_{\text{max}}=72000\text{r/min}$. Outside diameter of rotor is 59mm. The thickness of sleeve

is 1mm. $\Delta T=130^{\circ}\text{C}$. The magnets are evenly distributed along the circumference, thus achieving rotational symmetry without any bending effect. In this case, Equation (1-8) lead to satisfying results, which can be verified by an FE calculation. Using Equation (8), the ΔD is equal to 0.13mm. We can calculate the σ_{pre} , σ_{tem} , σ_{ω} are equal to 278MPa, 210MPa, 596MPa, respectively. And the $\rho_{N,\text{max}}$ is equal to 11.7MPa.

In order to verify the design method, the contact finite element method is used to calculation stress. The calculation results are shown in Figure 3. The stress caused by rotation and ΔT , ΔD are equal to 103MPa and 487MPa, respectively. The correctness of design method is verified by the results of FEA.

In order to limit the magnitude of air gap flux density harmonics, the new permanent magnet rotor structure 2 is designed with a pole coverage ratio of $\alpha < 1$ and shown in Figure 4.

This causes a considerable variation of radial bandage stress along the circumference, leading to additional bending forces in the carbon fiber. This bending stress is not included in Equation (1-8), so that more sophisticated calculations, considering also orthotropic behavior of the fiber material and bending forces, or FE calculations are required.

The calculation results of FEA are shown in Figure 5. The maximum stress in isotropic bandage is equal to 796MPa. But in the orthotropic bandage is equal to 924MPa. The calculation results have shown that the rotor has a very small tangential stress safety margin at the maximum speed. In fact, the new rotor crashed during a no-load test already at a rotational speed of 47 000r/min. According to the previous calculations, the rotor should have been able to withstand the mechanical stress at that speed.

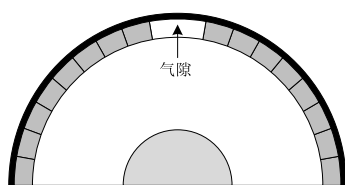


Figure 4. Structure of Permanent Magnet Rotor 2

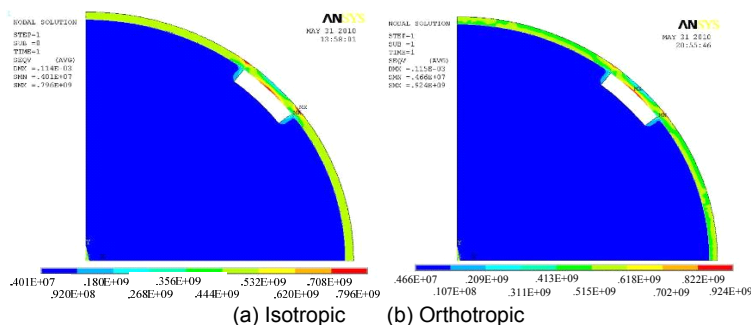


Figure 5. Stress Distribution

4. Strength Analysis of Buried Rotor

If the magnets are buried within the rotor iron, the rotor iron itself protects the magnets. The bandage is no needed, thus reducing the total air gap length. Exact analytical calculation of the mechanical stress inside the iron sheet is difficult. Therefore, the FEA calculation is recommended.

However, for simple magnet arrangements with buried permanent magnet rotor as shown in Figure 6, analytical approaches using an equivalent ring arrangement can still give a good estimate about the mechanical stress. The magnets are inserted into the slots, so no pre-stress is given. The outer iron bridge must withstand its own centrifugal forces and that of the magnets. Thermal expansion of iron and magnets is similar, so the temperature influence on stress is small. An analytical approach to calculate the mechanical stress on the rotor structure is shown in Figure 7.

The centrifugal forces acting on the magnets and the covering iron bridge are transferred to an equivalent ring with an artificially increased mass density ρ_{eq} . The height of the equivalent ring section h_r is chosen to be equal to the narrowest height of the iron bridge that covers the magnets. First, the increased mass density of the equivalent ring is determined as.

$$\rho_{\text{eq}} = \frac{\rho_m S_m + \rho_{\text{Fe}} S_{\text{Fe}}}{S_{\text{eq}}} \quad (9)$$

Both the masses of the magnet and the iron that covers the magnet are transformed into the equivalent ring. Thereby, it is assured that the equivalent ring suffers from the same centrifugal forces as the original arrangement. With the outer and inner radii of the equivalent ring, i.e., r_{ro} and r_{ri} , respectively, the tangential stress inside the equivalent ring under rotation at the maximum speed can be determined as.

$$\sigma_{eq} = \left(\frac{(r_{ro} + r_{ri})\pi n_{max}}{60} \right)^2 \rho_{eq} \quad (10)$$

So far, the calculation does not pay attention to local peak stress caused by the uneven distribution of the magnets and the shape of the magnet edges. By designing round-shaped slot edges, the increase of stress at these edges caused by the notch effect can be limited to about 100%. Therefore, the maximum mechanical stress is located at the slot edges, i.e.,

$$\sigma_{max} = 2\sigma_{eq} \quad (11)$$

The stress-strain characteristic of iron is nonlinear. The maximum tensile stress inside the iron must stay below the iron sheet yield strength $R_{p0.2}$. A typical value for $R_{p0.2}$, e.g., for M270-35A sheets, is $R_{p0.2}=450\text{N/mm}^2$. This means that putting a stress of $R_{p0.2}$ to the material will lead to a permanent relative deformation of 0.2%. This is accepted as permanent deformation of the iron sheets and therefore defines the limit of the stress that can be applied to the material. With special high-strength materials, yield strength can reach values of up to $R_{p0.2}=850\text{N/mm}^2$. Thus, the maximum permissible stress inside the rotor iron is:

$$\sigma_{max} < R_{p0.2} \quad (12)$$

The outside diameter of buried permanent magnet rotor is 63mm. Thickness of magnet is 2mm. The bridge of iron is 1mm. According to the previous explanations, this is also the value chosen for the height of the equivalent ring h_r . The cross-sectional area of one magnet and its covering iron amounts to the following equation.

$$S_{eq} = \pi(r_{ro}^2 - r_{ri}^2) / 4 = 48.67\text{mm}^2 \quad (13)$$

Hence, the mass density of the equivalent ring section is:

$$\rho_{eq} = 34907\text{kg} / \text{m}^3 \quad (14)$$

Finally, we get a tangential stress inside the equivalent ring due to rotation at the speed $n=50\ 000\text{r/min}$ of $\sigma_{eq}=918.74\text{MPa}$. Including the effect of the slot shape, the total tangential stress inside the rotor iron at the magnet edges will be $\sigma_{t,max}=1837\text{N/mm}^2$, which is far higher than the typical yield strength of the iron sheet material. This value would exceed the yield strength limit. The FE calculation resulted in maximum values for von Mises stress of 1890N/mm^2 shown in Figure 8.

As the value of the tangential stress clearly exceeds the yield strength limit $R_{p0.2}$ of typical electrical steel sheets. Equation (14) can also be used to determine the maximum permissible speed of buried rotor.

Considering the stress increase at the magnet edges, thus, for maximum permissible overspeed, we get $n_{max} = 26\ 082\text{r/min}$, which is far less than the maximum speed of a surface-mounted magnet rotor with a carbon-fiber bandage.

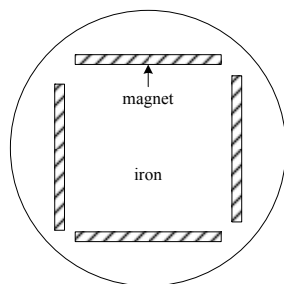


Figure 6. Structure of Buried Permanent Magnet Rotor

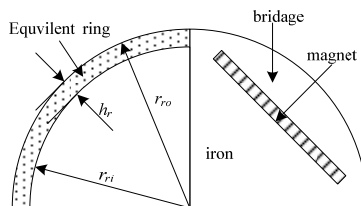


Figure 7. Equivalent Ring

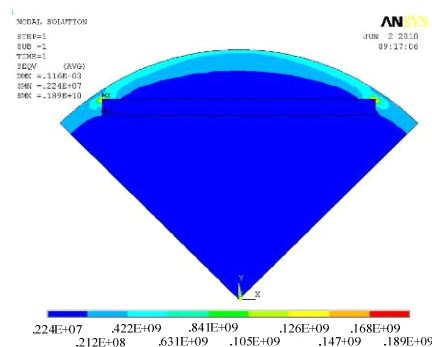


Figure 8. Stress Distribution

5. Conclusion

During the design of high-speed electrical machines, special attention needs to be paid to mechanical strength design issues. Although, in many cases, FE calculations for the mechanical strength of the rotor structure are recommended, for simple but realistic rotor structures, analytical approaches lead to satisfying results. This holds true both for surface-mounted and specially selected buried-magnet-type rotors. The fixation of magnets in surface-mounted and buried magnet-type high-speed permanent-magnet machines is compared for the same motor data, showing that for high-speed operation surface-mounted magnets fixed by a carbon-fiber bandage are the better choice, as they incorporate much higher mechanical strength and allowing higher maximum speed.

Acknowledgements

This work is supported by the Natural Science Foundations of Jiangsu Province (BK20130418), (BK2012462) and by the Natural Science Research Foundations of Jiangsu Province (13KJB470001).

References

- [1] Bianchi N, Bolognani S, Luise F. Potentials and limits of high-speed PM motors. *IEEE Transactions on Industry Applications*. 2004; 40(6): 1570-1578.
- [2] Jiabin C, Youguang G, Jianguo Z. Development of a High-Speed Permanent Magnet Brushless DC Motor for Driving Embroidery Machines. *IEEE Transactions on Magnetics* 2007; 43(11): 4004-4009.
- [3] Hanwook C, Kyoungjin K, Jangyong C, et al. Rotor Natural Frequency in High-Speed Permanent-Magnet Synchronous Motor for Turbo-Compressor Application. *IEEE Transactions on Magnetics*. 2011; 47(10): 4258-4261.
- [4] Pfister PD, Perriard Y. Very-High-Speed Slotless Permanent-Magnet Motors: Analytical Modeling, Optimization, Design, and Torque Measurement Methods. *IEEE Transactions on Industrial Electronics*. 2010; 57(1): 296-303.
- [5] Bailey C, Saban DM, Guedes Pinto P. Design of High-Speed Direct-Connected Permanent-Magnet Motors and Generators for the Petrochemical Industry. *IEEE Transactions on Industry Applications*. 2009; 45(3): 1159-1165.
- [6] Bernard N, Martin F, El-Hadi Zaïm M. Design Methodology of a Permanent Magnet Synchronous Machine for a Screwdriver Application. *IEEE Transactions on Energy Conversion*. 2012; 27(3): 624-633.
- [7] Do-Kwan H, Byung-Chul W, Ji-Young Lee, et al. Ultra High Speed Motor Supported by Air Foil Bearings for Air Blower Cooling Fuel Cells. *IEEE Transactions on Magnetics*. 2012; 48(2): 871-874.
- [8] Mirzaei M, Binder A, Funieru B. Analytical Calculations of Induced Eddy Currents Losses in the Magnets of Surface Mounted PM Machines With Consideration of Circumferential and Axial Segmentation Effects. *IEEE Transactions on Magnetics*. 2012; 48(12): 4831-4841.